Periodic sedimentation of three particles in periodic boundary conditions

M. L. Ekiel-Jeżewska[a)]
Institute of Fundamental Technological Research, Polish Academy of Sciences, Świętokrzyska 21,
00-049 Warsaw, Poland

B. U. Felderhof[b)]
Institut für Theoretische Physik A, Rheinisch-Westfälische Technische Hochschule Aachen,
Templergraben 55, 52056 Aachen, Germany

Solutions of the equations of Stokesian dynamics for point particles are found for periodic boundary conditions with three particles per unit cell of a simple cubic lattice. Two particles per cell move with equal velocity, but three particles per cell usually lead to irregular motion. For a class of initial conditions with special symmetry motions are found that are periodic in time as well as in space. It is shown that there is a range of stability in which the motions are robust under perturbation. © *2005 American Institute of Physics.* [DOI: 10.1063/1.2008827]

I. INTRODUCTION

The evolution and steady-state structure of sedimenting suspensions have recently been investigated by many authors.[1] The properties of such systems are determined by hydrodynamic interactions between individual particles, but collective effects play a dominant role. The interplay between the dynamics of small numbers of particles on the microscopic level and collective many-particle effects can be studied in spatially periodic systems with a small number of particles per unit cell. Instabilities of sedimenting infinite regular arrays of particles have been studied by Crowley.[2,3] Time-periodic stable motion of small clusters of particles in an infinite incompressible viscous fluid has been analyzed theoretically,[4–7] numerically,[8] and experimentally.[9] In the following we search for time-periodic stable motion of small clusters of particles in periodic boundary conditions. Periodic boundary conditions are widely used in numerical simulation of suspensions.[10,11]

Spatially periodic solutions of the steady-state Stokes equations for a viscous incompressible fluid were first studied by Hasimoto.[12] He considered regular arrays of spheres, in particular, the three cubic lattices, settling at constant speed under the influence of gravity. The fluid satisfies stick boundary conditions at the surface of each sphere. In the frame of the array the fluid moves on average with constant velocity, driven by a constant pressure gradient. Hasimoto, and later Zick and Homsy,[13] and Sangani and Acrivos,[14] calculated the friction per particle as a function of the sphere radius. In the following we consider systems with more than one particle per unit cell of a simple cubic lattice and find solutions of the Stokes equations, in combination with the equations of Stokesian dynamics, that are periodic in both space and time. For simplicity we restrict attention to the point particle limit, but it is clear that corresponding periodic solutions can be found for spheres.

Recently one of us studied linear waves in settling arrays

of point particles[15] and the corresponding question of stability of Hasimoto's solution. The linear wave solutions are periodic in space and time, but are limited to small amplitude. Here we consider large amplitude motions, but allow only a small number of particles per unit cell. The simplest case of two particles per unit cell is a direct generalization of Hasimoto's solution for point particles. We show that the pair settles steadily, with speed and direction depending on the relative distance of the pair in the basic unit cell.

For three particles per unit cell the motion becomes much more complicated[8] and cannot be found analytically. Numerically the motion is found to be irregular for most initial configurations. Special situations are of interest, where initially the distance vector of one pair is parallel to one of the horizontal axes of the cubic lattice and the members of this pair are at equal distance to the third particle. By symmetry the configuration keeps this character during the motion, and numerically the motion is found to be periodic. In our numerical work we have studied mostly the case where the initial triangle is horizontal and equilateral. Beyond a certain critical size we find solutions where the columns of horizontal pairs pass the columns of apex particles. We show that the periodic motion is neutrally stable for sizes of the initial triangle less than the critical size.

Similar periodic solutions for three point particles in infinite fluid were found by Hocking[4] and studied further by Caflisch, Lim, Luke, and Sangani.[5] Our solutions tend to theirs in the limit where the interparticle distances are much smaller than the lattice length. Golubitsky, Krupa, and Lim[6] have provided a mathematical study of sedimentation of clusters in infinite fluid in the point particle approximation, with particular emphasis on periodic solutions in the neighborhood of an equilibrium point where the particles settle without relative motion. A more detailed analysis of such periodic motions of three particles in infinite fluid has been given by Lim and McComb.[7] Much of both works can be transcribed to the case of periodic boundary conditions by the replacement of the Oseen tensor by the Hasimoto tensor.

[a)]Electronic mail: mekiel@ippt.gov.pl
[b)]Electronic mail: ufelder@physik.rwth-aachen.de

II. SEDIMENTATION IN PERIODIC BOUNDARY CONDITIONS

We consider sedimentation of a dilute system of identical spherical particles of radius a in a viscous incompressible fluid in periodic boundary conditions. In particular, we consider a simple cubic lattice of cells with side length L and volume $v_c = L^3$ per cell, and choose a Cartesian coordinate system with x, y, and z axes directed along the axes of the cubic lattice. There are N particles per unit cell, and a force $K = -Ke_z$ in the negative z direction acts on each particle. Particle configurations are repeated periodically in the cubic lattice. We shall consider the point limit $a \ll L$ and situations with at most four particles per unit cell.

The fluid velocity v and pressure p satisfy the linear Navier-Stokes equations,

$$\eta \nabla^2 v - \nabla p = -F(r), \quad \nabla \cdot v = 0, \tag{1}$$

where $F(r)$ is the force density acting on the fluid. In point approximation the force density is given by

$$F(r) = \sum_{n_j} K \delta(r - R_{n_j}), \tag{2}$$

where the sum is over the lattice cells, denoted by $n = (n_x, n_y, n_z)$ with n_x, n_y, and n_z running through all integers, and the N particles in each cell, labeled j. Again in point approximation, Hasimoto's solution[12] for fluid velocity and pressure takes the form

$$v_H(r) = -u_S + \sum_{j=1}^{N} \mathbf{T}_H(r - R_j) \cdot K,$$

$$\tag{3}$$

$$p_H(r) = \frac{N}{v_c} K \cdot r + \sum_{j=1}^{N} \mathbf{Q}_H(r - R_j) \cdot K,$$

where the positions $\{R_j\}$ are located in the basic unit cell. Furthermore, $v_c = L^3$ is the volume of the unit cell, and the Green functions $\mathbf{T}_H(r)$ and $\mathbf{Q}_H(r)$ have the periodicity of the lattice. The Hasimoto tensor $\mathbf{T}_H(r)$ is given by

$$\mathbf{T}_H(r) = \frac{1}{4\pi^2 \eta} \sum_{n}{}' \frac{1 - \hat{n}\hat{n}}{|n|^2} \exp[2\pi i n \cdot r], \tag{4}$$

where $\hat{n} = n/|n|$ and the prime on the summation sign indicates that the term $n = 0$ is omitted. An efficient scheme of numerical calculation of the Hasimoto tensor has been proposed by Cichocki and Felderhof.[16] The Hasimoto tensor has the property

$$\int_{v_c} \mathbf{T}_H(r) dr = 0, \tag{5}$$

so that $-u_S$ in Eq. (3) is the mean fluid velocity in the unit cell. To lowest order in the ratio a/L it is related to the force K by $K = \zeta u_S$, where $\zeta = 6\pi\eta a$ is the friction coefficient of a single particle. The Hasimoto tensor gives the additional flow pattern due to a single point particle and its periodic images. At small vector distance r the Hasimoto tensor becomes identical with the Oseen tensor $T(r)$ given by
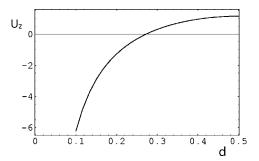

FIG. 1. Plot of the vertical velocity $U_z(d)$ of a pair of particles settling at constant distance D in the direction of the x axis in the unit cell of a simple cubic lattice with lattice distance L as a function of $d = D/L$.

$$T(r) = \frac{1}{8\pi\eta} \frac{1 + \hat{r}r}{r}. \tag{6}$$

Hasimoto considered a single particle per unit cell and calculated the tensor $\mathbf{T}_H(r)$ explicitly. In the chosen frame the single particle does not change position and may be taken at the origin.

For more than one particle per unit cell the instantaneous particle velocities are given by

$$u_j = -K \sum_{k \neq j}^{N} \mathbf{T}_H(R_j - R_k) \cdot e_z \quad (j = 1, \ldots, N) \tag{7}$$

and the configuration changes in time accordingly. The equations of motion of the Stokesian dynamics read

$$\frac{dR_j}{dt} = u_j(R_1, \ldots, R_N) \quad (j = 1, \ldots, N). \tag{8}$$

We recall that in the frame considered the mean fluid velocity is $-u_S$, so that in the frame where on average the fluid is at rest the velocity of particle j is $u_j + u_S$, with $u_S = K/6\pi\eta a$.

The Hasimoto tensor has the property

$$\mathbf{T}_H(r) = \mathbf{T}_H(-r), \tag{9}$$

so that, in particular, for two particles per unit cell with vector distance $r = R_1 - R_2$ the two velocities are equal

$$u_1 = u_2 = \mathbf{T}_H(r) \cdot K. \tag{10}$$

Hence the vector distance **r** remains constant in time, and the pair just translates at constant velocity. The same property holds for two particles in infinite fluid. Alternatively the pair motion may be viewed as the motion of two interlaced simple cubic lattices that do not move relative to each other. For more than two particles per unit cell the cubic lattices in general move relative to each other in complicated fashion. It clearly suffices to restrict attention to the motion of particles in the basic unit cell.

It is worthwhile to consider the common velocity of a pair as a function of distance. In Fig. 1 we plot the vertical velocity component U_z as a function of distance D in units $U_L = K/8\pi\eta L$ for two particles separated horizontally in the direction of the x axis. Of course, in this case the velocities $u_1 = u_2$ are directed vertically. On account of periodicity it suffices to consider distances less than $0.5L$. It is remarkable that for small distance D the velocity is downward, but for
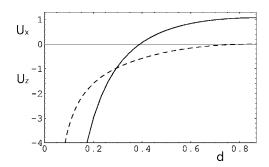
FIG. 2. Plot of the components $U_x(d) = U_y(d)$ (dashed curve) and $U_z(d)$ (solid curve) of the velocity of a pair separated at distance D in the direction of the body diagonal of the simple cubic lattice as a function of $d = D/L$.

$D > 0.2723L$ the velocity is upward. The reason is that the particles are slowed down due to the flow patterns of the periodic images. For the small distance $D = 0.1L$ the velocity is $U_z = -6.228 U_L$, compared to $U_{0z} = -10 U_L$ for two particles in infinite space, as calculated from the Oseen tensor $T(r)$, given by Eq. (6). The upward velocity for $D > 0.2723L$ means that in the frame of the fluid the pair moves at a speed less than the Stokes velocity of a single particle. Similar behavior is found for horizontal separations in other directions. For example, for the diagonal direction the velocity is upward for $D > 0.2702L$. A pair of particles separated along the vertical direction always moves downward, but again the velocity is smaller than for an isolated pair in infinite fluid. For example, for $D = 0.5L$ the velocity is $U_z = -1.9161 U_L$, compared to $U_{0z} = -4 U_L$ for the isolated pair.

We also consider a pair with distance vector directed along the body diagonal of the unit cell. This case is particularly interesting, since for $D = \frac{1}{2}\sqrt{3}L = 0.866L$ the configuration corresponds to a body-centered-cubic lattice. In Fig. 2 we plot the two components U_x and U_z of the common velocity as a function of separation D. The vertical component changes sign at $D = 0.3903L$. The horizontal component vanishes at $D = \frac{1}{2}\sqrt{3}L$. The vertical component then equals $U_z(\frac{1}{2}\sqrt{3}L) = 1.069\,248 U_L$. This corresponds precisely to the difference in velocity of the simple cubic and body-centered-cubic point lattices, as calculated by Hasimoto[12] for finite sphere radius a. The difference is given by

$$U_{\text{bcc}} - U_{\text{sc}} = -\frac{K}{6\pi\eta a}(Q_{\text{bcc}} - Q_{\text{sc}}), \qquad (11)$$

with Q factors given by, to order a/L,

$$Q_{\text{bcc}} = 1 - 1.791\,858\,5\,\phi^{1/3}, \quad Q_{\text{sc}} = 1 - 1.760\,118\,9\,\phi^{1/3}, \qquad (12)$$

where ϕ is the volume fraction occupied by particles, and the prefactors[17,18] correspond to the constant term in Hasimoto's function $S_1(r)$, as given in his Table 1. We have calculated the prefactors with greater accuracy than in Refs. 12 and 17. For a lattice with volume τ_0 of the unit cell the volume fraction is $\phi = 4\pi a^3/3\tau_0$. In our case the volume fraction of the simple cubic lattice is $4\pi a^3/3L^3$, and that of the body-centered lattice is $8\pi a^3/3L^3$. In the velocity difference in Eq. (11) the sphere radius a cancels, and one gets

$$
\begin{aligned}
U_{\text{bcc}} - U_{\text{sc}} &= \tfrac{4}{3}[1.791\,858\,5(8\pi/3)^{1/3} \\
&\quad - 1.760\,118\,9(4\pi/3)^{1/3}]U_L \\
&= 1.069\,248 U_L,
\end{aligned} \qquad (13)
$$

as found above from the motion of a pair.

Similarly we consider four particles in the basic unit cell positioned at time $t=0$ at the points $(0,0,0), (0.5,0.5,0)L, (0.5,0,0.5)L,$ and $(0,0.5,0.5)L$. This configuration corresponds to a face-centered-cubic lattice. One finds that the velocities of all four points are equal and directed in the z direction with value $U_z = 2.330\,086 U_L$. This may be compared again with Hasimoto's calculation of the mean fluid velocity to first order in a/L. As in Eq. (13) one finds

$$
\begin{aligned}
U_{\text{fcc}} - U_{\text{sc}} &= \tfrac{4}{3}[1.791\,747\,2(16\pi/3)^{1/3} \\
&\quad - 1.760\,118\,9(4\pi/3)^{1/3}]U_L = 2.330\,086 U_L,
\end{aligned} \qquad (14)
$$

in agreement with the motion of four particles in the simple cubic lattice.

III. THREE PARTICLES PER UNIT CELL

In this section we consider the motion of three particles in the basic unit cell of the simple cubic lattice. Explicitly the equations of motion read

$$\frac{d\boldsymbol{R}_1}{dt} = T_H(\boldsymbol{R}_1 - \boldsymbol{R}_2) \cdot \boldsymbol{K} + T_H(\boldsymbol{R}_1 - \boldsymbol{R}_3) \cdot \boldsymbol{K},$$

$$\frac{d\boldsymbol{R}_2}{dt} = T_H(\boldsymbol{R}_2 - \boldsymbol{R}_1) \cdot \boldsymbol{K} + T_H(\boldsymbol{R}_2 - \boldsymbol{R}_3) \cdot \boldsymbol{K},$$

$$\frac{d\boldsymbol{R}_3}{dt} = T_H(\boldsymbol{R}_3 - \boldsymbol{R}_1) \cdot \boldsymbol{K} + T_H(\boldsymbol{R}_3 - \boldsymbol{R}_2) \cdot \boldsymbol{K}. \qquad (15)$$

It is convenient to introduce the two relative coordinates

$$\boldsymbol{r}_1 = \boldsymbol{R}_3 - \boldsymbol{R}_1, \quad \boldsymbol{r}_2 = \boldsymbol{R}_2 - \boldsymbol{R}_1. \qquad (16)$$

These satisfy the equations of motion,

$$\frac{d\boldsymbol{r}_1}{dt} = T_H(\boldsymbol{r}_1 - \boldsymbol{r}_2) \cdot \boldsymbol{K} - T_H(\boldsymbol{r}_2) \cdot \boldsymbol{K},$$

$$\frac{d\boldsymbol{r}_2}{dt} = T_H(\boldsymbol{r}_1 - \boldsymbol{r}_2) \cdot \boldsymbol{K} - T_H(\boldsymbol{r}_1) \cdot \boldsymbol{K}. \qquad (17)$$

We shall consider solutions with special symmetry for which the initial triangle is isosceles with the unequal side parallel to either the x axis or the y axis. It follows from symmetry that the triangle retains these properties in the course of time. Without loss of generality we choose the point $\boldsymbol{R}_2$ as the apex and the vector $\boldsymbol{r}_1$ parallel to the x axis. Besides the reflection symmetry shown in Eq. (9) the Hasimoto tensor has the symmetry properties

$$T_{Hxz}(-x,y,z) = -T_{Hxz}(x,y,z),$$

$$T_{Hyz}(-x,y,z) = T_{Hyz}(x,y,z),$$

$$T_{Hzz}(-x,y,z) = T_{Hzz}(x,y,z),$$ (18)

as well as

$$T_{Hxz}(x,y,-z) = -T_{Hxz}(x,y,z),$$

$$T_{Hyz}(x,y,-z) = -T_{Hyz}(x,y,z),$$ (19)

$$T_{Hzz}(x,y,-z) = T_{Hzz}(x,y,z).$$

In particular, in the xy plane,

$$T_{Hxz}(x,y,0) = T_{Hyz}(x,y,0) = 0.$$ (20)

For the isosceles triangles under consideration the relative coordinates $\boldsymbol{r}_1$ and $\boldsymbol{r}_2$ can be expressed as

$$\boldsymbol{r}_1 = (2x_2,0,0), \quad \boldsymbol{r}_2 = (x_2,y_2,z_2),$$ (21)

with three independent coordinates (x_2,y_2,z_2). It is easily seen that for $\boldsymbol{K} = -K\boldsymbol{e}_z$ the equations of motion (17) reduce to

$$\frac{dx_2}{dt} = KT_{Hxz}(x_2,y_2,z_2), \quad \frac{dy_2}{dt} = -KT_{Hyz}(x_2,y_2,z_2),$$ (22)

$$\frac{dz_2}{dt} = KT_{Hzz}(2x_2,0,0) - KT_{Hzz}(x_2,y_2,z_2).$$

In infinite fluid the same equations hold with the Hasimoto tensor $\boldsymbol{T}_H$ replaced by the Oseen tensor $\boldsymbol{T}$ given by Eq. (6). In that case there is a constant of the motion, $x_2(t)y_2(t) = A$, first found by Hocking.[4] This implies geometrically that the area of the triangle spanned by the three points projected on a horizontal plane remains constant in time. In periodic boundary conditions this constant does not apply, and the solution of the three coupled equations (22) must be found.

In our numerical work we consider, in particular, situations for which the initial triangle is horizontal and equilateral. By translational invariance one of the corners may be taken to be at the origin, so that we may choose as initial configuration the points $(0,0,0),(D/2,D\sqrt{3}/2,0)$, and $(D,0,0)$, labeled as 1, 2, and 3. By symmetry the side 13 remains parallel to the x axis in the course of time, and the triangle remains isosceles with equal sides 12 and 23, but it does not remain horizontal. At the initial time the three velocities are directed in the z direction, but the velocity of the apex particle 2 differs from that of particles 1 and 3. The coordinates x_2, y_2, and z_2 introduced in Eq. (21) take the values $(D/2,D\sqrt{3}/2,0)$ at time $t=0$.

Numerically we find that for $d = D/L < 0.4242$ the solution $[x_2(t),y_2(t),z_2(t)]$ of Eq. (22) is purely periodic. For $d > 0.4242$ the coordinate $z_2(t)$ has an additional linear contribution $U_z t$. The period $T(d)$ can be determined from the periodic motion of $x_2(t)$ or $y_2(t)$. The velocity U_z then follows from
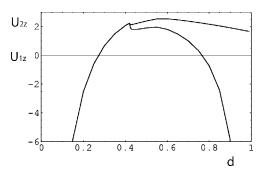

FIG. 3. Plot of the average vertical velocities $U_{1z}(d)$ (lower curve) and $U_{2z}(d)$ (upper curve) of two of the particles at the corners of a triangle that is initially horizontal and equilateral with side length $D=dL$.

$$U_z = \frac{K}{T}\int_0^T \{T_{Hzz}[2x_2(t),0,0] - T_{Hzz}[x_2(t),y_2(t),z_2(t)]\}dt$$ (23)

and is found to equal $U_z = L/T$. Hence the motion $z_2(t)$ modulo L is also periodic.

The positions of particles 1 and 2 at time t are found from Eq. (15) as

$$\boldsymbol{R}_1(t) = \boldsymbol{R}_1(0) + \int_0^t \{\boldsymbol{T}_H[\boldsymbol{r}_1(t)] + \boldsymbol{T}_H[\boldsymbol{r}_2(t)]\} \cdot \boldsymbol{K}dt,$$

$$\boldsymbol{R}_2(t) = \boldsymbol{R}_2(0) + \int_0^t \{\boldsymbol{T}_H[\boldsymbol{r}_2(t)] + \boldsymbol{T}_H[\boldsymbol{r}_1(t) - \boldsymbol{r}_2(t)]\} \cdot \boldsymbol{K}dt$$ (24)

and similarly for particle 3. The motion with the above initial condition is periodic in the horizontal directions. The vertical motion is a superposition of a periodic motion with the same period and a linear motion, so that each of the three particles performs a spiraling motion. There are now two steady velocities $U_{1z} = U_{3z}$ and U_{2z}. From Eqs. (15) and (16) we have

$$U_{1z} = -\frac{K}{T}\int_0^T \{T_{Hzz}[\boldsymbol{r}_1(t)] + T_{Hzz}[\boldsymbol{r}_2(t)]\}dt$$ (25)

and similarly

$$U_{2z} = -\frac{K}{T}\int_0^T \{T_{Hzz}[\boldsymbol{r}_2(t)] + T_{Hzz}[\boldsymbol{r}_1(t) - \boldsymbol{r}_2(t)]\}dt.$$ (26)

These are the time-averaged particle velocities in the chosen frame, where the mean fluid velocity is $-u_S\boldsymbol{e}_z$. Both velocities are equal for $d < 0.4242$. Since $U_{2z} - U_{1z} = U_z$ we have

$$(U_{2z} - U_{1z})T = nL,$$ (27)

with $n=0$ for $d < 0.4242$ and $n=1$ for $d > 0.4242$.

In Fig. 3 we plot the two velocities U_{1z} and U_{2z} as functions of dimensionless distance $d = D/L$. We call $d_0 = 0.4242$ the doubling point. In Fig. 4 we plot the period T as a function of d. It follows from Eq. (27) that the period diverges at $d = d_0+$. Numerically it diverges also at $d = d_0-$. The difference of steady velocities for $d > d_0$ implies that during a period the columns of particles labeled as 1 and 3 pass the columns labeled as 2. One can determine the two velocities numerically very accurately by plotting the projection of a
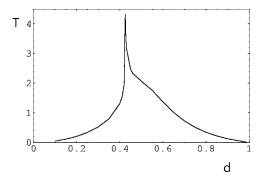
FIG. 4. Plot of the period $T(d)$ of the motion of three particles that are initially at the corners of a horizontal equilateral triangle with side length $D=dL$.

FIG. 6. Plot of the motion of three particles that are initially at the corners of a horizontal equilateral triangle with side length $D=dL$ for $d=0.42$. The triangle formed by the particle positions is shown at times $t=0,T/4,T/2,3T/4,T$. The motion is in the upward direction in the frame in which a single particle per unit cell would be motionless.

spiral on a vertical plane and adjusting the velocity of the coordinate frame in the vertical direction until one gets a closed curve.

There are two more special points in Fig. 3. At $d=0.2712$ the common velocity $U_{1z}=U_{2z}$ turns from negative to positive. For $d<0.2712$ the triangle moves down faster than a single particle and slower for $0.2712<d<d_0$. For $d>d_0$ the motion changes in character, and one has passing columns. For $d_0<d<0.7674$ the three particles on average move slower than a single particle would, and for $0.7674<d<1$ only the apex particle 2 on average moves slower than a single particle, but particles 1 and 3 move faster. The last feature can be understood from the proximity of particles in the neighboring cells at the left and right, giving rise to fast moving pairs. For d close to unity the velocity of the pair 1,3 is predominantly in the $-z$ direction and much larger than the velocity of particle 2. Hence the period of motion is determined by the average speed of the fast close pair in nearly rectilinear motion, and Eq. (27) is satisfied with $n=1$. For the largest value of d considered, $d=0.99$, we indeed find $n=1$.

At the doubling point the motion changes significantly. Not only are there two distinct steady velocities U_{z1} and U_{z2} for $d>d_0$, but the amplitude of the deviation from steady motion also increases. In Fig. 5 we plot the projection of the
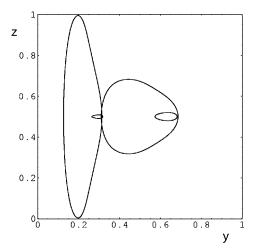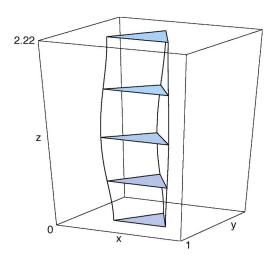
points $\mathbf{R}_1(t)$ and $\mathbf{R}_2(t)$ onto the yz plane during one period for initial equilateral triangles of sides $d=0.42$ and $d=0.43$, with the steady displacement subtracted for both particles. The amplitude for $d=0.42$ is much smaller. In Fig. 6 we show the positions of the triangle with sides $d=0.42$ at $t=0$ for times $t=0,\frac{1}{4}T,\frac{1}{2}T,\frac{3}{4}T,T$. In Fig. 7 we show the corresponding triangles for $d=0.43$ at $t=0$.

We consider again the more general case of isosceles triangles. We denote the solution of the equations of motion (22) with initial conditions $x_2(0)=x_{20}$, $y_2(0)=y_{20}$, and $z_2(0)=0$ as $r_{2h}(t)$. It depends parametrically on the initial values (x_{20},y_{20}). The solution has the properties

$$x_{2h}(-t)=x_{2h}(t), \quad x_{2h}(t+T)=x_{2h}(t),$$

$$y_{2h}(-t)=y_{2h}(t), \quad y_{2h}(t+T)=y_{2h}(t), \tag{28}$$

FIG. 5. Plot of the projection on the yz plane of the periodic deviation from uniform motion for $d=0.420$ (small figures) and $d=0.430$ (large figures).
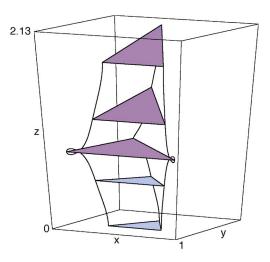

FIG. 7. As in Fig. 6 for $d=0.43$.

TABLE I. List of values characterizing the motion of three point particles that are initially at the corners of a horizontal equilateral triangle with side length $D=dL$. The period T is measured in units $8\pi\eta L^2/K$, the velocities U_{z1} and U_{z2} are measured in units $U_K=K/8\pi\eta L$, and the distances x_{20} and y_{20} are measured as fractions of L. The remaining quantities are dimensionless and explained in Eq. (31).

d	T	U_{z1}	U_{z2}	x_{20}	ρ_{x1}	ρ_{x2}	y_{20}	ρ_{y1}	ρ_{y2}	Δ_z
0.1	0.050	−12.455	−12.455	0.05	1.000	1.000	0.087	1.000	1.000	0
0.2	0.212	−2.528	−2.528	0.1	1.001	1.002	0.173	0.999	0.998	0
0.3	0.531	0.654	0.654	0.15	1.007	1.014	0.260	0.993	0.986	0.003
0.4	1.321	2.060	2.060	0.2	1.053	1.107	0.346	0.957	0.915	0.019
0.42	1.952	2.220	2.220	0.21	1.111	1.205	0.364	0.916	0.851	0.027
0.425	4.317	1.894	2.125	0.2125	1.280	1.931	0.368	0.806	0.485	−0.237
0.43	3.197	1.815	2.128	0.215	1.247	1.902	0.372	0.828	0.495	−0.219
0.45	2.464	1.793	2.199	0.225	1.211	1.791	0.390	0.860	0.542	−0.186
0.5	2.063	1.896	2.380	0.25	1.181	1.525	0.433	0.910	0.712	−0.122
0.6	1.371	1.802	2.532	0.3	1.107	1.218	0.520	1.016	1.038	−0.044
0.7	0.729	1.000	2.372	0.35	1.056	1.109	0.606	1.030	1.062	−0.020
0.8	0.346	−0.729	2.158	0.4	1.025	1.045	0.693	1.017	1.032	−0.009
0.9	0.129	−5.839	1.909	0.45	1.006	1.011	0.779	1.005	1.010	−0.003

$$z_{2h}(-t) = -z_{2h}(t), \quad z_{2h}(t+T) = nL + z_{2h}(t),$$

with period $T(x_{20}, y_{20})$ depending on the initial position in the plane $z_2=0$. These properties follow from the symmetries given by Eqs. (9), (18), and (19). We recall that $U_z(x_{20}, y_{20}) = nL/T(x_{20}, y_{20})$.

An approximate representation of the relative motion is given by

$$x_{2c}(t) = x_{21} + (x_{20} - x_{21})\cos(2\pi t/T),$$

$$y_{2c}(t) = y_{21} + (y_{20} - y_{21})\cos(2\pi t/T),$$

$$z_{2c}(t) = U_z t + (z_{21} - nL/4)\sin(2\pi t/T),$$

with the abbreviation $r_{21} = r_{2h}(T/4)$. We also denote $r_{22} = r_{2h}(T/2)$. The approximate representation (29) uses a single harmonic and the symmetry properties (28). The actual motion is anharmonic. The approximation described by Eq. (29) has been chosen such that at the beginning and end of each period, and at one-quarter of the period, the particle positions coincide with those of the actual motion. By symmetry the positions then coincide at three quarters of the period as well. The approximate motion described by Eq. (29) takes place in the vertical plane given by the equation

$$\frac{x_2 - x_{21}}{x_{20} - x_{21}} = \frac{y_2 - y_{21}}{y_{20} - y_{21}}. \tag{30}$$

In this plane and in a frame moving with velocity U_z in the vertical direction the approximate motion is along an ellipse centered at $(x_{21}, y_{21}, U_z t)$. A measure of the deviations from the approximate orbit given by Eq. (29) is found by comparison of the actual values at half period r_{22} with the corresponding $r_{2c}(T/2)$. We define

$$\rho_{xj} = \frac{x_{2j}}{x_{20}}, \quad \rho_{yj} = \frac{y_{2j}}{y_{20}}, \quad j = 1, 2, \tag{31}$$

$$\Delta_z = (z_{21} - (1/4)nL)/L.$$

Here $2x_{20} = d$ is the width of the triangle at time $t=0$, when it is horizontal and isosceles, and ρ_{x1} is the ratio of the width at one-quarter of the period to the initial width. Similarly ρ_{x2} is the ratio of the width at half period to the initial width. Furthermore y_{20} is the height of the triangle at time $t=0$, and ρ_{y1} is the ratio of the projection of the height on the horizontal plane at one-quarter of the period to the initial height. Similarly ρ_{y2} is the ratio of the projection of the height at half period to the initial height. We note that it follows from Eq. (28) that $z_{2h}(T-t) = nL - z_{2h}(t)$, so that at half the period $z_{2h}(T/2) = nL/2$. In particular, for the purely periodic motions with $U_z = 0$ at half period $z_{2h}(T/2) = 0$. Finally, Δ_z is a measure of the rise of the apex above the horizontal plane at one-quarter of the period, with the steady motion subtracted. In Table I we list typical values for the orbits corresponding to triangles that are initially horizontal and equilateral with sides d. Similar data are easily obtained for triangles that are initially isosceles.

IV. STABILITY

In this section we analyze the stability of the periodic motion of three points initially forming an isosceles horizontal triangle with unequal side parallel to the x axis. To investigate stability it suffices to study the relative motion of particles. We consider first the equations of motion (22). These equations correspond to a limited class of perturbed motions in which the triangles remain isosceles with unequal side parallel to the x axis. The motion described by Eq. (22) numerically appears to be orbitally stable, since the orbits are periodic in space and depend continuously on the initial conditions in the horizontal plane at $z=0$, except at a doubling point ($d=d_0$ for the equilateral triangle). On the other hand, the relative motion of three points described by Eq. (17) can still be unstable, since a wider class of perturbations is allowed. In particular, for points initially at the vertices of equilateral triangles the motion described by Eq. (17) is un-

stable when the sides of the initial triangle are larger than d_0L, even though Eq. (22) implies stability. Stability of the motions considered can be investigated by the method of the Floquet theory.[19]

In preparation of the study of Eq. (17) we first apply the Floquet theory to the motion described by Eq. (22). We denote the solution of the equations of motion (22) for which we wish to investigate stability by $r_2^*(t)$. A solution of Eqs. (22) with slightly different initial conditions is expressed as

$$r_2(t) = r_2^*(t) + \xi(t). \tag{32}$$

Linearizing Eq. (22) for small deviations $\xi(t)$ we obtain a set of three linear equations of motion. In vector form

$$\frac{d\xi}{dt} = A(t) \cdot \xi(t), \tag{33}$$

with time-dependent 3×3 matrix $A(t)$ given by

$$A(t) = \begin{pmatrix} P_{2xx}(t) & P_{2xy}(t) & P_{2xz}(t) \\ -P_{2yx}(t) & -P_{2yy}(t) & -P_{2yz}(t) \\ 2P_{1zx}(t) - P_{2zx}(t) & -P_{2zy}(t) & -P_{2zz}(t) \end{pmatrix}, \tag{34}$$

where the 3×3 matrix $P_2(t)$ is given by $P_2(t) = P[r_2^*(t)]$ with the tensor $P(r)$ defined in terms of derivatives of the Hasimoto tensor as

$$P_{\alpha\beta}(r) = K \frac{\partial T_{H\alpha z}(r)}{\partial r_\beta}, \tag{35}$$

with $(\alpha, \beta) = (x, y, z)$. From the symmetry properties (28) of the solution $r_2^*(t)$ and the properties (18) and (19) of the Hasimoto tensor it follows that

$$P_{2\alpha\beta}(t) = -P_{2\alpha\beta}(T-t) \text{ for } (\alpha\beta) = (xx),(yy),(xy),(yx),(zz), \tag{36}$$

$$P_{2\alpha\beta}(t) = P_{2\alpha\beta}(T-t) \text{ for } (\alpha\beta) = (xz),(zx),(yz),(zy).$$

The 3×3 matrix $P_1(t)$ is defined by $P_1(t) = P[r_1^*(t)]$ with $r_1^*(t) = [2x_2^*(t), 0, 0]$. Only the elements $P_{1xz}(t)$ and $P_{1zx}(t)$ of this matrix are nonvanishing, and they have the properties $P_{1xz}(t) = P_{1xz}(T-t)$ and $P_{1zx}(t) = P_{1zx}(T-t)$.

In the Floquet theory[19] a set of three independent solutions of Eq. (33) is collected in the fundamental matrix $\Phi_3(t)$ that is the solution of the matrix equation

$$\frac{d\Phi_3}{dt} = A(t) \cdot \Phi_3(t), \tag{37}$$

with initial condition $\Phi_3(0) = I_3$, where I_3 is the 3×3 identity matrix. The characteristic matrix E_3 is defined by

$$E_3 = \Phi_3(T). \tag{38}$$

The motion $r_2^*(t)$ is unstable if some of the eigenvalues of E_3 are greater than unity in absolute value. In our case we find that the three eigenvalues equal unity. This is an example of a situation sometimes called neutrally stable.[20] By definition neutral stability means that the absolute value of each eigenvalue is not larger than unity. The nature of the characteristic matrix can be argued from the geometrical properties of the solutions as follows.

We can make the dependence of the solution $r_2(t)$ on the initial conditions $r_2(0) = r_{20}$ explicit by writing the solution as $r_2(r_{20}, t)$. With this notation the matrix $\Phi_3(t)$ can be expressed as

$$\Phi_3(t) = \left. \frac{\partial r_2(r_{20}, t)}{\partial r_{20}} \right|_{r_2^*}. \tag{39}$$

In words, the matrix $\Phi_3(t)$ incorporates the ratio of the difference of solutions after time t to small variations of the initial conditions in the direction of the x_2, y_2, and z_2 axes. The initial condition $\Phi_3(0) = I$ is clearly satisfied. We consider, in particular, the solution $r_2^*(t) = r_{2h}(t)$, defined above Eq. (28), which passes through the plane $z_2 = 0$ at time $t = 0$. It follows from Eqs. (20) and (22) that for this solution the velocity vector $v_2(t) = dr_2(t)/dt$ is perpendicular to the plane $z_2 = 0$ at times $t = 0$ and $t = T$. Consider first the neighboring orbit corresponding to an infinitesimal change dx_{20} of the initial point in the x_2 direction. For the purely periodic motions the point is back at its initial position after a time $T(x_{20} + dx_{20}, y_{20})$. The difference in position with the point $(x_{20}, y_{20}, 0)$ after time $T(x_{20}, y_{20})$ arises from the difference in orbit and from the difference in period. To first order the point at time $T(x_{20}, y_{20})$ has x_2 and y_2 coordinates $(x_{20} + dx_{20}, y_{20})$, but z_2 coordinate given by the partial derivative $-\partial T(x_{20}, y_{20})/\partial x_{20}$ times the velocity component $v_{2z}(T) = v_{2z}(0)$. Similar considerations hold for changes of the initial point in the y_2 direction. A change in the z_2 direction simply corresponds to a shift along the original orbit. Hence the matrix E_3 takes the form

$$E_3 = \begin{pmatrix} 1 & 0 & 0 \\ 0 & 1 & 0 \\ Q_x & Q_y & 1 \end{pmatrix}, \tag{40}$$

with Q_x and Q_y given by $-v_{2z}(0)\partial T(x_{20}, y_{20})/\partial x_{20}$ and $-v_{2z}(0)\partial T(x_{20}, y_{20})/\partial y_{20}$, respectively. The matrix E_3 clearly has three eigenvalues equal to unity. Similar considerations hold for the solutions of Eq. (22) for which U_z equals L/T.

The matrix $A(t)$ in Eq. (37) is periodic in time, $A(t+T) = A(t)$, and the fundamental matrix $\Phi_3(t)$ satisfies[19]

$$\Phi_3(t+T) = \Phi_3(t) \cdot E_3. \tag{41}$$

The fundamental matrix has columns $\Phi_3(t) = [f_1(t), f_2(t), f_3(t)]$ consisting of solutions of Eq. (33) satisfying the initial conditions

$$f_1(0) = \begin{pmatrix} 1 \\ 0 \\ 0 \end{pmatrix}, \quad f_2(0) = \begin{pmatrix} 0 \\ 1 \\ 0 \end{pmatrix}, \quad f_3(0) = \begin{pmatrix} 0 \\ 0 \\ 1 \end{pmatrix}. \tag{42}$$

It follows from Eqs. (40) and (41) that these solutions have the properties

$$f_1(t+T) = f_1(t) + Q_x T f_3(t),$$

$$f_2(t+T) = f_2(t) + Q_y f_3(t), \quad f_3(t+T) = f_3(t). \tag{43}$$

Hence $f_3(t)$ is periodic, but $f_1(t)$ and $f_2(t)$ are not. We note that the solution $f_3(t)$ can be identified with $f_3(t) = v_2(t)/v_{2z}(0)$. The linear combinations

$$\boldsymbol{\psi}(t) = Q_y \boldsymbol{f}_1(t) - Q_x \boldsymbol{f}_2(t),$$

$$\boldsymbol{\phi}(t) = \frac{Q_x}{Q_x^2 + Q_y^2} \boldsymbol{f}_1(t) + \frac{Q_y}{Q_x^2 + Q_y^2} \boldsymbol{f}_2(t) - \frac{t}{T} \boldsymbol{f}_3(t). \tag{44}$$

clearly are periodic, and satisfy the differential equations

$$\frac{d\boldsymbol{\psi}}{dt} = \boldsymbol{A}(t) \cdot \boldsymbol{\psi}(t), \quad \frac{d\boldsymbol{\phi}}{dt} = \boldsymbol{A}(t) \cdot \boldsymbol{\phi}(t) - \frac{1}{T} \boldsymbol{f}_3(t). \tag{45}$$

Solving Eq. (44) for $\boldsymbol{f}_1(t)$ and $\boldsymbol{f}_2(t)$ one finds

$$\boldsymbol{f}_1(t) = \frac{Q_y}{Q_x^2 + Q_y^2} \boldsymbol{\psi}(t) + Q_x \left[\boldsymbol{\phi}(t) + \frac{t}{T} \boldsymbol{f}_3(t) \right],$$

$$\boldsymbol{f}_2(t) = \frac{-Q_x}{Q_x^2 + Q_y^2} \boldsymbol{\psi}(t) + Q_y \left[\boldsymbol{\phi}(t) + \frac{t}{T} \boldsymbol{f}_3(t) \right]. \tag{46}$$

Hence the solutions $\boldsymbol{f}_1(t)$ and $\boldsymbol{f}_2(t)$ grow approximately linearly with time. The growth is due to the dependence of the period T on (x_{20}, y_{20}), as for Poincaré stable periodic orbits.[19] The properties derived above are confirmed by numerical calculation.

In order to study stability under a wider class of perturbations we must return to the equations of motion (17). We denote the periodic solution of these equations corresponding to initial conditions of a horizontal isosceles triangle at $t=0$ by $[\boldsymbol{r}_1^*(t), \boldsymbol{r}_2^*(t)]$, with again $\boldsymbol{r}_1^*(t) = [2x_2^*(t), 0, 0]$. A solution of Eqs. (17) with slightly different initial conditions is expressed as

$$\boldsymbol{r}_1(t) = \boldsymbol{r}_1^*(t) + \boldsymbol{\xi}_1(t), \quad \boldsymbol{r}_2(t) = \boldsymbol{r}_2^*(t) + \boldsymbol{\xi}_2(t). \tag{47}$$

Linearizing Eqs. (17) for small deviations $\boldsymbol{X}(t) = [\boldsymbol{\xi}_1(t), \boldsymbol{\xi}_2(t)]$ we obtain a set of six linear equations of motion. In vector form

$$\frac{d\boldsymbol{X}}{dt} = \boldsymbol{B}(t) \cdot \boldsymbol{X}(t), \tag{48}$$

with time-dependent 6×6 matrix $\boldsymbol{B}(t)$ given by

$$\boldsymbol{B}(t) = \begin{pmatrix} -\boldsymbol{P}_{12}(t) & \boldsymbol{P}_{12}(t) + \boldsymbol{P}_2(t) \\ -\boldsymbol{P}_{12}(t) + \boldsymbol{P}_1(t) & \boldsymbol{P}_{12}(t) \end{pmatrix}, \tag{49}$$

with $\boldsymbol{P}_{12}(t) = \boldsymbol{P}[\boldsymbol{r}_1^*(t) - \boldsymbol{r}_2^*(t)]$. A set of six independent solutions of Eq. (48) is collected in the fundamental matrix $\boldsymbol{\Phi}_6(t)$ that is the solution of the matrix equation

$$\frac{d\boldsymbol{\Phi}_6}{dt} = \boldsymbol{B}(t) \cdot \boldsymbol{\Phi}_6(t), \tag{50}$$

with initial condition $\boldsymbol{\Phi}_6(0) = \boldsymbol{I}_6$, where $\boldsymbol{I}_6$ is the 6×6 identity matrix. The characteristic 6×6 matrix $\boldsymbol{E}_6$ equals $\boldsymbol{\Phi}_6(T)$, as in Eq. (38). The numerical integration of Eq. (50) becomes numerically inaccurate near the doubling point. This is related to the fact that the multipliers (Q_x, Q_y) diverge at the transition point, as is evident from the expressions given below Eq. (40) and the fact that the period T diverges at the transition.

We can improve the analysis by making use of symmetries. It is easily shown that the matrix $\boldsymbol{P}_1(t)$ has the properties

$$P_{1xx}(t) = P_{1xy}(t) = P_{1yx}(t) = P_{1yy}(t) = P_{1zz}(t) = 0, \tag{51}$$

and that the matrices $\boldsymbol{P}_{12}(t)$ and $\boldsymbol{P}_2(t)$ are related by

$$\begin{pmatrix} P_{12xx} & P_{12xy} & P_{12xz} \\ P_{12yx} & P_{12yy} & P_{12yz} \\ P_{12zx} & P_{12zy} & P_{12zz} \end{pmatrix} = \begin{pmatrix} -P_{2xx} & P_{2xy} & P_{2xz} \\ P_{2yx} & -P_{2yy} & -P_{2yz} \\ P_{2zx} & -P_{2zy} & -P_{2zz} \end{pmatrix}. \tag{52}$$

As a consequence, five of the elements of the 3×3 matrix in the upper right-hand corner of the matrix $\boldsymbol{B}(t)$ in Eq. (48) vanish. By a similarity transformation $\boldsymbol{B}'(t) = \boldsymbol{S} \cdot \boldsymbol{B}(t) \cdot \boldsymbol{S}^{-1}$ we can obtain an even simpler matrix of the form

$$\boldsymbol{B}'(t) = \begin{pmatrix} \boldsymbol{C}(t) & \boldsymbol{0} \\ \boldsymbol{D}(t) & \boldsymbol{A}(t) \end{pmatrix}. \tag{53}$$

The 6×6 matrix $\boldsymbol{S}$ can be taken to have the form

$$\boldsymbol{S} = \begin{pmatrix} 1 & 0 & 0 & -2 & 0 & 0 \\ 0 & 1 & 0 & 0 & 0 & 0 \\ 0 & 0 & 1 & 0 & 0 & 0 \\ b & 0 & 0 & 1-2b & 0 & 0 \\ 0 & 0 & 0 & 0 & 1 & 0 \\ 0 & 0 & 0 & 0 & 0 & 1 \end{pmatrix}, \tag{54}$$

with any value of b. The 3×3 matrix $\boldsymbol{C}(t)$ in Eq. (53) then has elements

$$\boldsymbol{C} = \begin{pmatrix} -P_{2xx} & P_{2xy} & P_{2xz} - 2P_{1xz} \\ -P_{2yx} & P_{2yy} & P_{2yz} \\ -P_{2zx} & P_{2zy} & P_{2zz} \end{pmatrix}. \tag{55}$$

Evidently the solution $\boldsymbol{\Phi}_6'(t)$ of the transformed Eq. (50) takes the same form as the matrix $\boldsymbol{B}'(t)$ in Eq. (53). Therefore three eigenvalues of the transformed characteristic matrix $\boldsymbol{E}_6'$ have already been found from the solution of Eq. (37) and are equal to unity. The remaining three eigenvalues can be found from the solution of the three equations,

$$\frac{d\boldsymbol{\Phi}_3'}{dt} = \boldsymbol{C}(t) \cdot \boldsymbol{\Phi}_3'(t). \tag{56}$$

In this way the eigenvalues of $\boldsymbol{E}_6'$ are found with greater numerical accuracy than from Eq. (50). The product of the eigenvalues is exactly equal to unity, because the integral of $\mathrm{Tr}\,\boldsymbol{C}(t)$ over the period vanishes,[19] as follows from the symmetry properties (36). For the triangles that are initially equilateral with base parallel to one of the axes of the periodic cube we find numerically that for $d < d_0$ the three eigenvalues of the matrix $\boldsymbol{E}_3'$ corresponding to the solution of Eq. (56) are numerically equal to unity. For $d > d_0$ one of the eigenvalues is larger than unity. The analysis shows that the solution of Eq. (17) for such initial triangles is neutrally stable for $d < d_0$ and unstable for $d > d_0$. Numerically this is noticeable by the fact that the solution of Eqs. (17) becomes irregular after a limited number of periods. For $d < 0.4242$ we find numerically that the motion remains periodic for many periods.

V. DISCUSSION

We have found interesting solutions of the equations of the Stokesian dynamics for point particles in periodic boundary conditions. If there are two particles per unit cell of a simple cubic lattice they move steadily with equal velocity. Three particles per unit cell move in complicated fashion, usually irregularly, but solutions periodic in time can be found for initial conditions with symmetry corresponding to that of the lattice. We have investigated numerically the periodic motion of three point particles located initially at the vertices of an equilateral horizontal triangle with one side parallel to the x axis of the cubic cell. For triangles with side dL less than a critical size $d_0 L$ the motion is neutrally stable.

Such stable solutions of the equations of the Stokesian dynamics are of relevance to the theory of sedimentation. In these solutions the particles move coherently in complicated fashion with the same mean sedimentation velocity and a periodic internal motion of the three-particle cluster. If initially the particles are sufficiently widely separated, but the motion is still stable, the mean sedimentation velocity is less than that of a single particle. In this case the solution describes a situation of hindered settling.

If the initial equilateral triangle is too large, with side length $dL > d_0 L$, the two base particles team up with partners in neighboring cells, and we get separate motion of a base pair and a single particle with different mean vertical velocities and with periodic motions superimposed. The corresponding solutions are unstable.

Since in computer simulations often periodic boundary conditions are employed, the solutions found here may provide a useful test for the algorithms used. Clearly it would be of interest to extend the calculation to equal-sized spheres with radius comparable to the lattice distance. Since such situations involve the same symmetries as for point particles, we may expect periodic solutions of similar nature. Although the hydrodynamic interactions for spheres are far more difficult to treat, we expect that a calculation employing the method of induced force multipoles[21] is feasible. Caflisch, Lim, Luke, and Sangani,[5] have extended the calculation for three point particles in infinite space to three equal-sized spheres.

[1] S. Ramaswamy, "Issues in the statistical mechanics of steady sedimentation," Adv. Phys. **50**, 297 (2001).

[2] J. M. Crowley, "Viscosity-induced instability of one-dimensional lattice of falling spheres," J. Fluid Mech. **45**, 151 (1971).

[3] J. M. Crowley, "Clumping instability of a falling horizontal lattice," Phys. Fluids **19**, 1296 (1976).

[4] L. M. Hocking, "The behaviour of clusters of spheres falling in a viscous fluid. Part 2. Slow motion theory," J. Fluid Mech. **20**, 129 (1964).

[5] R. E. Caflisch, C. Lim, J. H. C. Luke, and A. S. Sangani, "Periodic solutions for three sedimenting spheres," Phys. Fluids **31**, 3175 (1988).

[6] M. Golubitsky, M. Krupa, and C. Lim, "Time-reversibilty and particle sedimentation," SIAM J. Appl. Math. **51**, 49 (1991).

[7] C. C. Lim and I. H. McComb, "Stability of normal modes and subharmonic bifurcations in the 3-body Stokeslet problem," J. Diff. Eqns. **121**, 384 (1995).

[8] I. M. Jánosi, T. Tél, D. E. Wolf, and J. A. C. Gallas, "Chaotic particle dynamics in viscous flows: The three-particle Stokeslet problem," Phys. Rev. E **56**, 2858 (1997).

[9] K. O. L. F. Jayaweera, B. J. Mason, and G. W. Slack, "The behaviour of clusters of spheres falling in a viscous fluid. Part 1. Experiment," J. Fluid Mech. **20**, 121 (1964).

[10] A. Sierou and J. F. Brady, "Accelerated Stokesian dynamics simulations," J. Fluid Mech. **448**, 115 (2001).

[11] A. J. C. Ladd, "Dynamical simulation of sedimenting spheres," Phys. Fluids A **5**, 299 (1993).

[12] H. Hasimoto, "On the periodic fundamental solution of the Stokes equations and their application to viscous flow past a cubic array of spheres," J. Fluid Mech. **5**, 317 (1959).

[13] A. A. Zick and G. M. Homsy, "Stokes flow through periodic array of spheres," J. Fluid Mech. **115**, 13 (1982).

[14] A. S. Sangani and A. Acrivos, "Slow flow through a periodic array of spheres," Int. J. Multiphase Flow **8**, 343 (1982).

[15] B. U. Felderhof, "Mesoscopic stability and sedimentation waves in settling periodic arrays," Phys. Rev. E **68**, 051402 (2003).

[16] B. Cichocki and B. U. Felderhof, "Periodic fundamental solution of the linear Navier-Stokes equations," Physica A **159**, 19 (1989).

[17] R. A. Coldwell-Horsfall and A. A. Maradudin, "Zero-point energy of an electron lattice," J. Math. Phys. **1**, 395 (1960).

[18] B. R. A. Nijboer, "On a relation between the scattering cross-section in dense media and the energy of a dilute electron gas," Philips Res. Rep. **30**, 74 (1975).

[19] D. W. Jordan and P. Smith, *Nonlinear Ordinary Differential Equations* (Clarendon, Oxford, 1987), p. 245.

[20] M. Golubitsky and D. G. Schaeffer, *Singularities and Groups in Bifurcation Theory* (Springer, Berlin, 1985), Vol. 1, p. 362.

[21] B. Cichocki, B. U. Felderhof, K. Hinsen, E. Wajnryb, and J. Bławzdziewicz, "Friction and mobility of many spheres in Stokes flow," J. Chem. Phys. **100**, 3780 (1994).